SMR/406-23

THIRD AUTUMN WORKSHOP ON ATMOSPHERIC RADIATION AND CLOUD PHYSICS
27 November - 15 December 1989

"Principles of Remote Sensing of Atmospheric Parameters from Space"

Rolando RIZZI
L.M.D./C.N.R.S.
Dipartimento di Fisica
Bologna
Italy

Principles of Remote Sensing of Atmospheric Parameters from Space

Rolando Rizzi

Dipartimento di Fisica, Bologna, Italy

1. Introduction

The interaction of electromagnetic radiation with matter modifies to some extent the incident wave. The medium therefore produces a signature in the amplitude, phase or spectral composition which depends on its composition and structure. The basic principle associated with remote sensing of the atmospheric temperature and humidity structure involves the interpretation of radiometric measurements of electromagnetic radiation in specific spectral intervals which are sensitive to some physical aspects of the medium. More specifically, at any wavenumber (or wavelength) in the infrared or microwave regions where an atmospheric constituent absorbs radiation, it also emits thermal radiation according to Kirchoff's Law. Since the radiance leaving the atmosphere is a function of the distribution of the emitting gases and the distribution of temperature throughout the atmosphere, measurements of radiance contain some information on both these quantities. Meaurements by satellite instruments using this principle have used two distinct kinds of viewing geometry:

- a. near-nadir viewing in which radiation is observed leaving the atmosphere in directions near the local vertical;
- b. the limb view in which radiation leaving the atmosphere nearly tangentially is observed.

The lecture will deal with the problem associated to the retrieval of temperature and humidity profiles from nadir-view radiances.
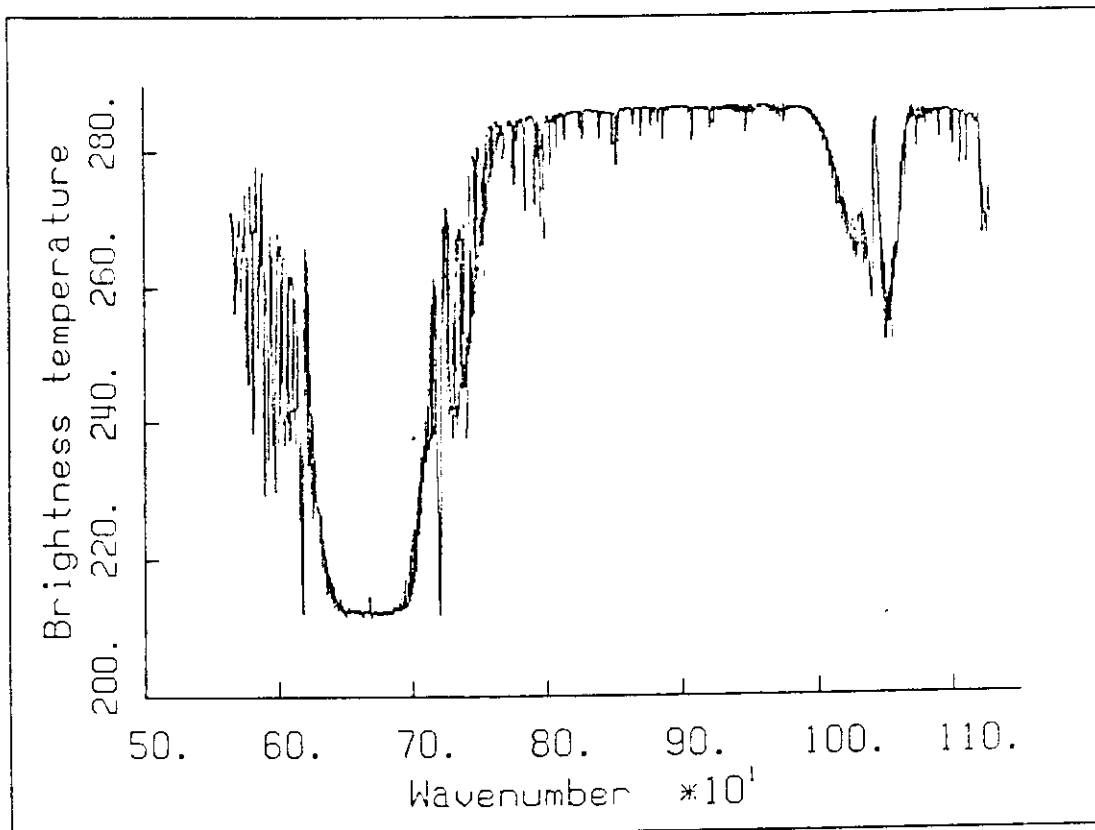
Figure 2.1

2. Spectral distribution of radiance leaving the atmosphere.

The amount of energy per unit area per unit solid angle per unit spectral interval (centered around a given wavenumber) as measured by a radiometer on board a satellite, looking downward to the atmosphere, is termed upwelling radiance with units $[Wm^{-2}ster^{-1}cm^{-1}]$. The same amount of energy can also be defined in terms of the temperature of a perfectly black body yelding the same radiance in the same wavenumber interval. The latter quantity is referred to as brightness temperature $(T_B\ [K])$. Piots of T_B, obtained from atmospheric emitted radiance measured at 10 km by a radiometer looking vertically downward, are shown in Fig. 2.1. versus wavenumber ν expressed in units of cm^{-1}.

The spectral range shown in the figure covers an important domain used for atmospheric sounding purposes, namely the window region from 1050 to 770 cm^{-1} (about 9.5 to 13 μm) and the whole CO_2 absorption band centered at 672 cm^{-1} (15 μm). Another important feature is the ozone absorption band around 1040 cm^{-1} (9.6 μm). Reminding that low values of T_B are associated to low numeric values of radiances, it appears that some complex interaction is taking place within the atmosphere producing large variations in energy emitted upwards. An explanation for this requires some knowledge in basic spec-

troscopy, the principles of which will be dealt with in next section. Furthermore it may be noted that T_B attains minimum values in regions where the CO_2 molecules produce large absorption (for example around 670 cm^{-1}) while largest (warmest) T_B are measured in regions where the atmosphere is particularly transparent, the absorption by water vapour being very small. It may be noticed that a constant T_B corresponds to diminishing values of radiance as we move to higher wavenumbers since the maximum value for the Planck function at 300 K is around 600 cm^{-1}.

In next section it will be shown that the presence of sharp variations in brightness temperature (or radiance, or absorption properties) is due to the nature of the interaction which is quantized.

3. Modelling the interaction.

For interaction to take place a force must act on a molecule in presence of an external electromagnetic field. The existence of such a force depends on the presence of an electric or magnetic instantaneous dipole moment. The polarizability of a molecule is related to the extent to which a molecule has a permanent dipole moment or can acquire an oscillating one produced by its vibrational motion. If we consider a molecule as a rigid rotator, radiative interaction can take place only if the molecule possess a permanent dipole moment. Thus CO, N_2O, H_2O and O_3 (see Fig. 3.1) interact with the field by changing their "rotation vector" while N_2, O_2, CO_2 and CH_4 do not. However as a molecule like CO_2 vibrates, an oscillating electrical dipole moment is produced and rotational interaction can take place. Hence CO_2 and CH_4 possess vibration-rotational couplings with the incident wave.

In what follows only interaction trought electric dipole moments will be considered, the main aim of this section being to show some examples of how molecular absorption and emission spectra can be explained (and computed).

A. The molecule as a rigid quantized rotator.

Diatomic or linear triatomic molecule (Fig 3.2) have two equal moments of inertia and two degrees of rotational freedom. Asymmetric top molecules, like H_2O have three unequal moments of inertia and three degrees of freedom.

The kinetic energy E_{rot} of a rigid rotator is $E_{rot} = \frac{1}{2}I\omega^2$. While for a classical rotator ω and hence E_{rot} can take any value, a quantized rotator is subject to quantum restrictions on angular momentum

$$I\omega = \frac{h}{2\pi}[J(J+1)]^{1/2}$$

where J, the quantum number for rotation, can assume only integer values. The quantized rotational energy can therefore be written
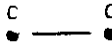
3
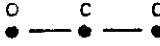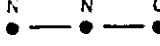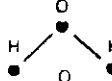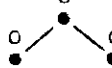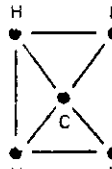
Molecule   Arrangement   Permanent
Dipole Moment

N₂ ... No

O₂ ... No

CO ... Yes

CO₂ ... No

N₂O ... Yes

H₂O ... Yes

O₃ ... Yes

CH₄ ... No

Figure 3.1. Symbolic nuclear configurations and permanent dipole moment status of some atmospheric molecules.

Linear diatomic: N_2, O_2, CO, NO

Linear triatomic: CO_2, NO_2, N_2O

c.g.

Asymmetric top (bent triatomic): H_2O, O_3

c.g.

Figure 3.2. Axes of rotational freedom for linear and asymmetric top molecules.

4

$$E_J = E_{rot.J} = \frac{1}{2}\frac{(I\omega)^2}{I} = \frac{h^2}{8\pi^2 I}J(J+1)$$

Recalling that E_J is the rotational energy associated to a rotational state J around a specific principal axis and calling rotational constant the quantity

$$A = \frac{h}{8\pi^2 c I_A}$$

where I_A is the moment of inertia around that axis, we may write

$$E_J = Ahc\ J(J+1)$$

In analogy, for asymmetric top molecules we will have three moments of inertia (I_A, I_B, I_C) and three rotational constants (namely A, B and C). The rotational energy can be expressed in terms of the rotational term $F(J)$

$$F(J) = \frac{E_j}{hc} = BJ(J+1)$$
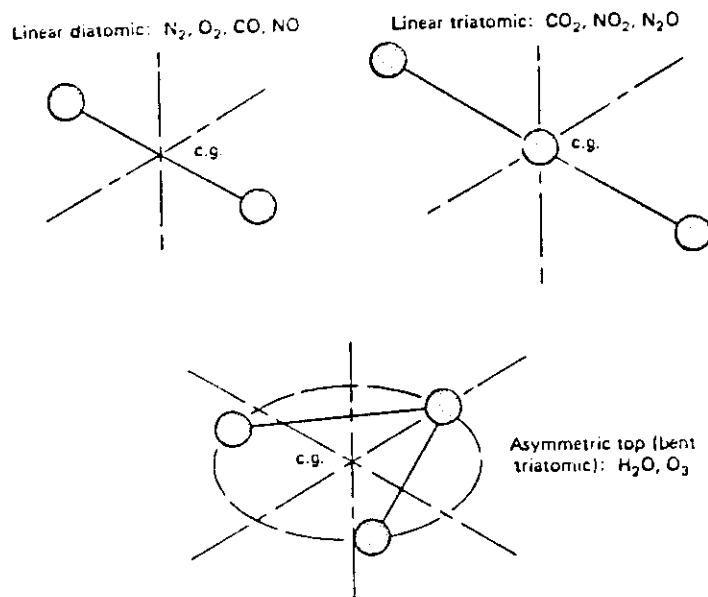
which is measured in the energy unit cm^{-1}.

In Table 3.1 values of the molecular electrical dipole and rotational constants for some of the most important active atmospheric species are given.

Table 3.1.

Values of molecular electrical dipole (moment μ in Debye units) and rotational constants of some atmospheric molecules

Species	μ	A	B	C
CO	0.112	–	1.9314	–
CO_2	0.	–	0.3902	–
N_2O	0.167	–	0.4190	–
H_2O	1.85	27.877	14.512	9.285
O_3	0.53	3.553	0.445	0.395
CH_4	0.	–	5.249	–

Interaction between the molecule and the external field takes place whenever a quantum of energy $h\nu c$ is extracted (absorption process) or added (emission) to the external field. The basic relation holds

5

$$E' - E'' = h\nu c$$

where E' and E'' are the two energy levels involved. Denoting the upper and lower rotational quantum number as J' and J'' the difference bewtween the two energy levels is

$$\Delta F = BJ'(J' + 1) - BJ''(J'' + 1)$$

A quantum selection rule dictates that only transition among adjacent levels are allowed, that is

$$\Delta J = J' - J'' = \pm 1$$

where the value $\Delta J = +1$ applies to absorption, which increases the internal energy of the molecule. Hence for the case of absorption

$$\Delta F = 2B(J'' + 1) = 2BJ' = \nu_{rot} \tag{3.1}$$

The absorbed photons have energies that are individually equal to Eq. (3.1) and the aggregate effect from all the molecules in a volume is a depletion of the incident wave energy at wavenumber ν_{rot} which is observed as a spectral line.

As an example absorption of a photon at wavenumber 669.29 (corresponding to the wavelength 14.947 μm is accomplished by the H_2O molecule spinning around its principal axis A with a transition from rotational quantum number 12 to 13. The line can be seen in the detailed spectrum of Fig. 3.3.

B. The molecule as a quantized vibrator.

An ensemble of nuclear masses held together by elastic valence bonds forms a system capable of vibrating in one or more modes. Some of the most commonly encountered vibrational modes for biatomic and triatomic molecules are shown in Fig. 3.4.

A classical two-mass vibrator has a natural frequency $\tilde{\nu}$ which is given by

$$\tilde{\nu} = \frac{1}{2\pi} \left(\frac{k}{m'}\right)^{1/2}$$

where k is the elastic force constant and m' is the reduced mass. The potential energy for this system is given by the relation

$$E_p = 2\pi^2 m'(r - r_0)^2 \tilde{\nu}^2$$

where r_0 id the distance between the two masses at equilibrium. Quantum restrictions on vibrational energy are found by solving the time independent Schroedinger equation in one dimension. The eigenvalues defining the allowed energy levels are
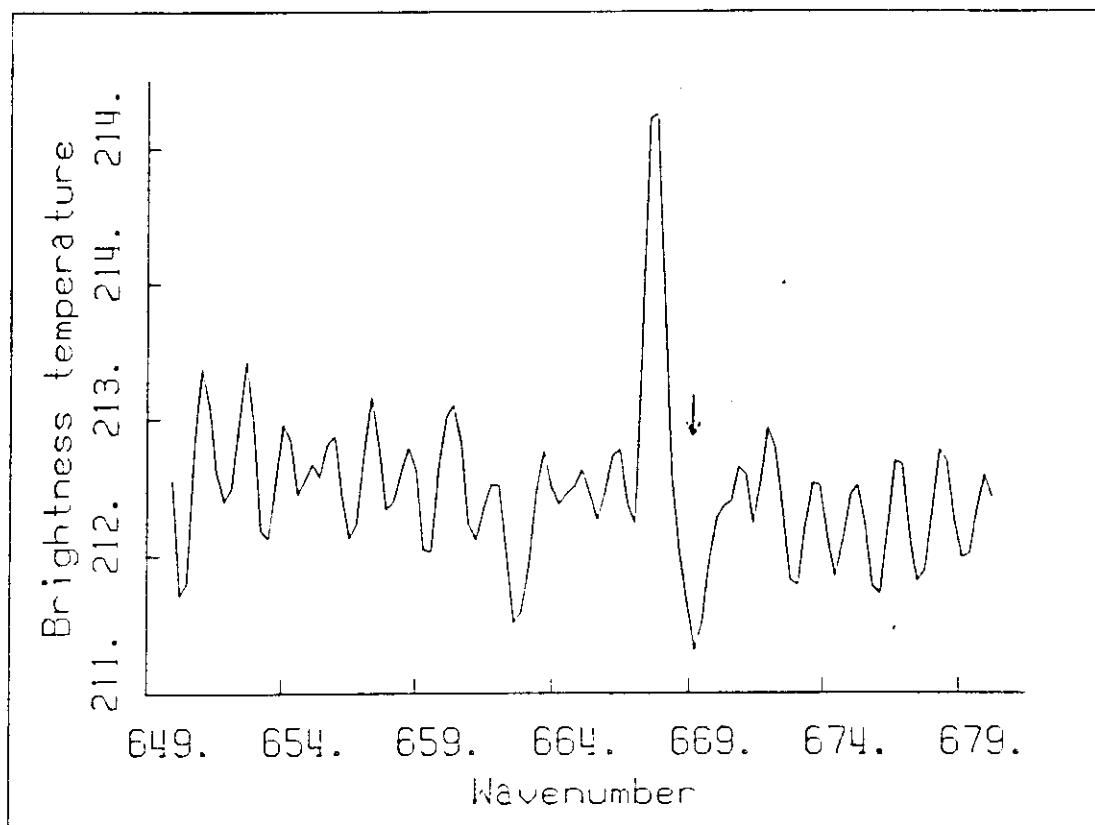
Figure 8.3. High resolution (about half wavenumber) brightness temperature spectrum from 650 to 680 wavenumbers. The arrow points at the water vapour absorption line referred to in the text.
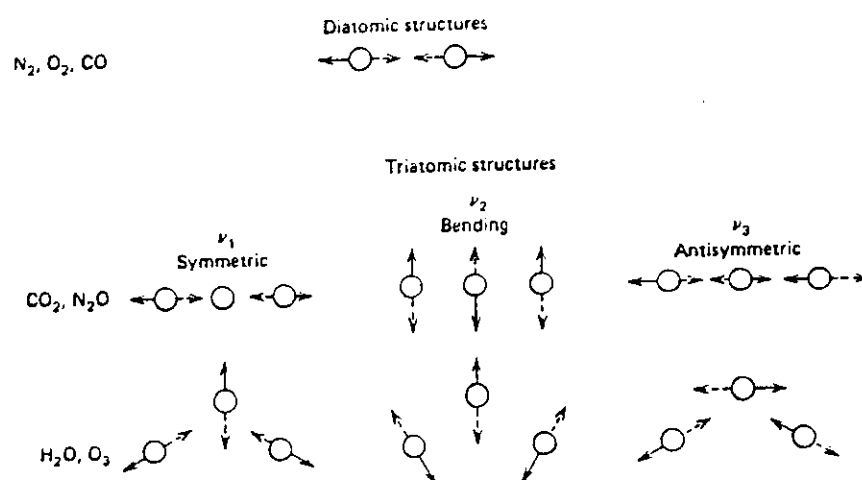

Figure 8.4. Symbolic configurations and vibrational modes of diatomic and triatomic molecules.

$$E_\nu = (v + \frac{1}{2})h\tilde{\nu} \qquad v = 0, 1, 2, \ldots$$

$$E_\nu = (v + \frac{1}{2})\frac{h}{2\pi}\left(\frac{k}{m'}\right)^{1/2}$$

where v is the quantum number for vibration. These equations hold for a simple harmonic motion, which is true only when the vibrational quantum number is small. Disregarding some of the complexities of real life, we may consider a simple transition of a diatomic molecule from two adjacent vibrational levels since the quantum selection rule allows only transition for which $\Delta v = \pm 1$, where the plus sign applies for transition in which the internal energy is incremented through absorption of a quantum of energy. Denoting by v' any level except $v = 0$ and by v'' the next lower level, the transition energy is

$$\Delta E = \frac{h}{2\pi}\left(\frac{k}{m'}\right)^{1/2}\left[(v' + \frac{1}{2}) - (v'' + \frac{1}{2})\right]$$

hence

$$\Delta E = \frac{h}{2\pi}\left(\frac{k}{m'}\right)^{1/2}$$

Therefore a photon of energy $h\nu_{vib}/c$, where ν_{vib} denotes the wavenumber of the transition, will be absorbed if

$$\Delta E = h\tilde{\nu} = h\nu_{vib}c$$

that is when

$$\nu_{vib} = \frac{1}{2\pi c}\left(\frac{k}{m'}\right)^{1/2}$$

The absorption by a volume of gas will result in the depletion of radiation of wavenumber ν_{vib} (or frequency $\tilde{\nu}$) which appears as an absorption line in the spectrum. As an example let's consider the CO molecule. Its reduced mass is $m' = 1.14 \times 10^{-23}$ grams and the force constant has a value of $k = 1.84 \times 10^6 \ dyn\,cm^{-1}$. Substituting these values in the last equation we obtain for a transition from level $v = 0$ to $v = 1$ an energy increase $\Delta E = 4.24 \times 10^{-23} \ ergs$ equivalent to $\nu_{vib} = 2143\,cm^{-1}$. In Table 3.2 the vibrational frequencies, wavelengths and wavenumbers of interesting atmospheric radiative molecules are listed.

C. Vibro-rotational bands.

It has been already pointed out that molecules not possessing a permanent dipole moment do in fact possess oscillating dipole moments, caused by their vibrational motion,

8

Vibrational frequencies, wavelengths and wavenumbers of radiatively active atmospheric molecules.

Species	Parameter	Vibrational Modes		
		ν_1	ν_2	ν_3
CO	Hz	6.43×10^{13}	—	—
	μm	4.67	—	—
	cm^{-1}	2143	—	—
CO$_2$	Hz	—	2.00×10^{13}	7.05×10^{13}
	μm	—	15.0	4.26
	cm^{-1}	—	667	2349
N$_2$O	Hz	3.86×10^{13}	1.77×10^{13}	6.67×10^{13}
	μm	7.78	17.0	4.49
	cm^{-1}	1285	589	2224
H$_2$O	Hz	1.10×10^{14}	4.79×10^{13}	1.13×10^{14}
	μm	2.73	6.27	2.65
	cm^{-1}	3657	1595	3776
O$_3$	Hz	3.33×10^{13}	2.12×10^{13}	3.13×10^{13}
	μm	9.01	14.2	9.59
	cm^{-1}	1110	705	1043
NO	Hz	5.71×10^{13}	—	—
	μm	5.25	—	—
	cm^{-1}	1904	—	—
NO$_2$	Hz	3.92×10^{13}	2.26×10^{13}	4.86×10^{13}
	μm	7.66	13.25	6.17
	cm^{-1}	1306	755	1621
CH$_4$	Hz	8.75×10^{13}	4.60×10^{13}	9.06×10^{13}
	μm	3.43	6.52	3.31
	cm^{-1}	2917	1534	3019
		ν_4		
CH$_4$	Hz	5.71×10^{13}		
	μm	5.25		
	cm^{-1}	1904		

and therefore rotational transition coupled to vibrational transition are possible. Considering a simple molecule with one degree of rotational freedom (CO_2 for example) we may therefore observe absorption (and emission) corresponding to quantum energies

$$\Delta E = h\nu c = \Delta E_{vib} + \Delta E_{rot}$$

where the terms on the right side are taken with their sign. That is a number of transition are allowed depending on the number of degrees of rotational freedom and on the number of vibrational modes. A simple description of the allowed energy transitions are shown in Fig.3.5.

The more complex the molecular structure the larger the number of possible transitions. As an example Fig. 3.6 shows the superposition of NO rotational lines close to the vibrational wavenumber at ≈ 1904 cm^{-1} with a resolution of 0.06 cm^{-1} while in Fig. 3.7 the complex structure due to the three rotational modes of NO_2 is superimposed to its
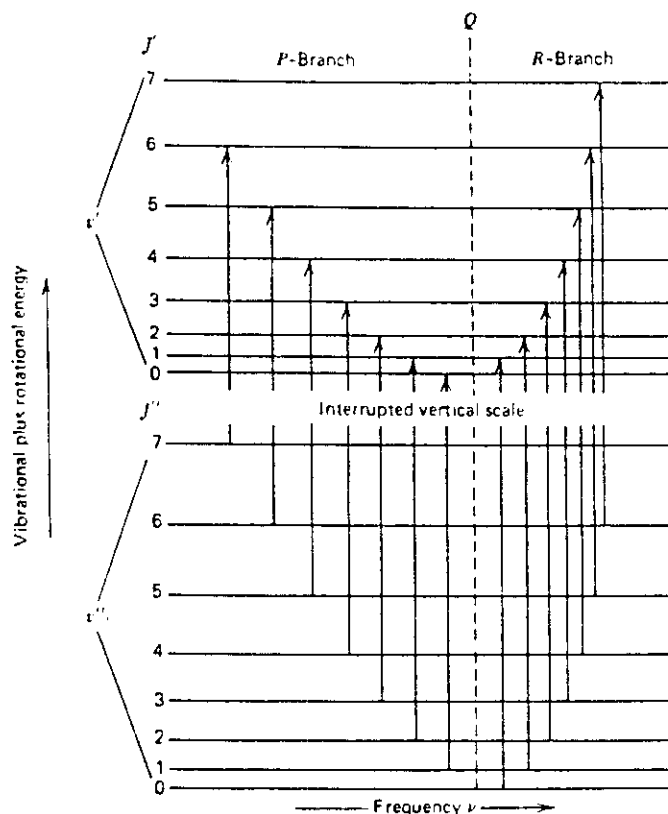
Figure 3.5. Simultaneous transitions in vibrational and rotational energies.

vibrational transition at $\approx 1621\ cm^{-1}$. In the latter the resolution of the measurements is $0.02\ cm^{-1}$.

Water vapour is one of the most important radiatively active molecules. Its complicated rotational (three degrees of freedom) and vibrational (three modes) structure produce a line spectrum which, at first sight, appears randomly distributed. One of the most important H_2O absorption feature is the vibro-rotational band at $\approx 1595\ cm^{-1}$ shown in Fig 3.8.

At longer wavelengths, micro and millimeter-wave frequencies, single rotational lines are also observed. Three of these, due to H_2O and O_2, are going to play an increasingly important role in remote sensing, namely the line centered at 64 and 112 (O_2) and 183 (H_2O) Ghz which are shown in Fig. 3.9.
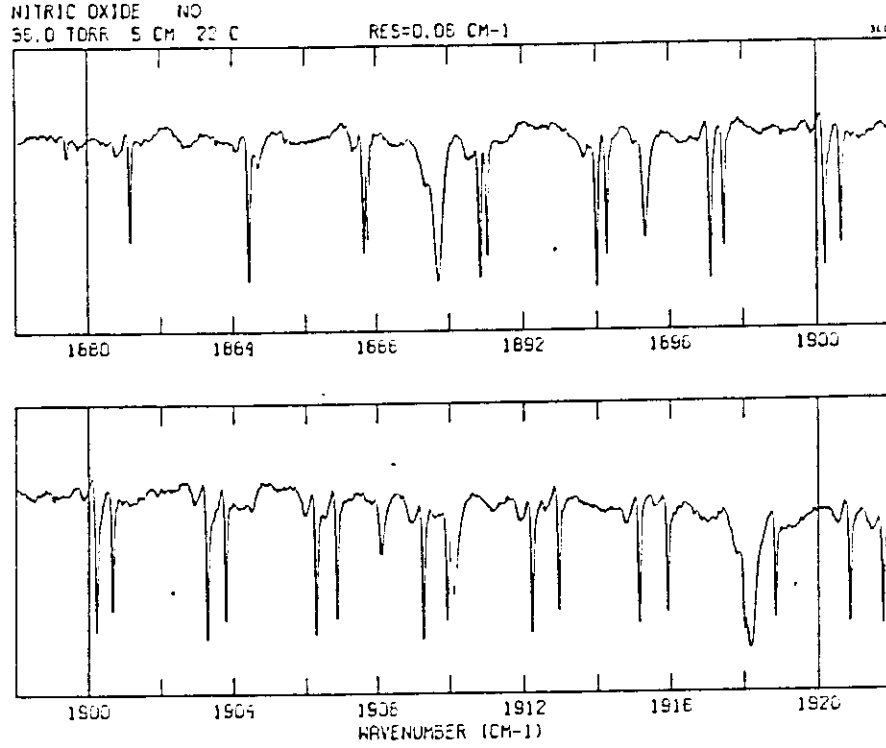
Figure 8.6. Nitric oxide spectrum .

4. The direct problem.

The equation of radiative transfer at the upper boundary of the atmosphere, describes the relation between the outgoing radiances and atmospheric parameters. For a cloudless atmosphere it can be approximately written in the form

$$L_\nu(\vartheta) = \varepsilon B_\nu(T_s)\tau_\nu(p_s, \vartheta) + L_\nu^\uparrow(\vartheta) + (1 - \varepsilon)L_\nu^\downarrow(\vartheta)\tau_\nu(p_s, \vartheta) \tag{4.1}$$

$$L_\nu^\uparrow(\vartheta) = \int_{p_s}^0 B_\nu(T(p))\frac{\partial \tau_\nu(p, \vartheta)}{\partial \ln p} \, d\ln p \tag{4.2}$$

$$L_\nu^\downarrow(\vartheta) = \int_0^{p_s} B_\nu(T(p))\frac{\partial \tau_\nu'(p, \vartheta)}{\partial \ln p} \, d\ln p \tag{4.3}$$

where $L_\nu(\vartheta)$ is the radiance (subscript ν, wavenumber, indicates that monochromatic quantities are involved), ε is the emissivity of the lower surface, $T(p)$ is the vertical profile of absolute temperature, $q(p)$ is the vertical profile of mass mixing ratio of the absorbing (emitting) material (water vapour, CO_2, N_2O, ozone, etc.), ϑ is the sensing angle, $B(T)$ is the Planck function, $\tau(p, \vartheta) \equiv \tau(p, \vartheta; T, q)$ and is $\tau'(p, \vartheta) \equiv \tau'(p, \vartheta; T, q)$ are the transmittance functions respectively from the top of the atmosphere to the level at pressure p and from level p to the lower boundary, and are expressed by:
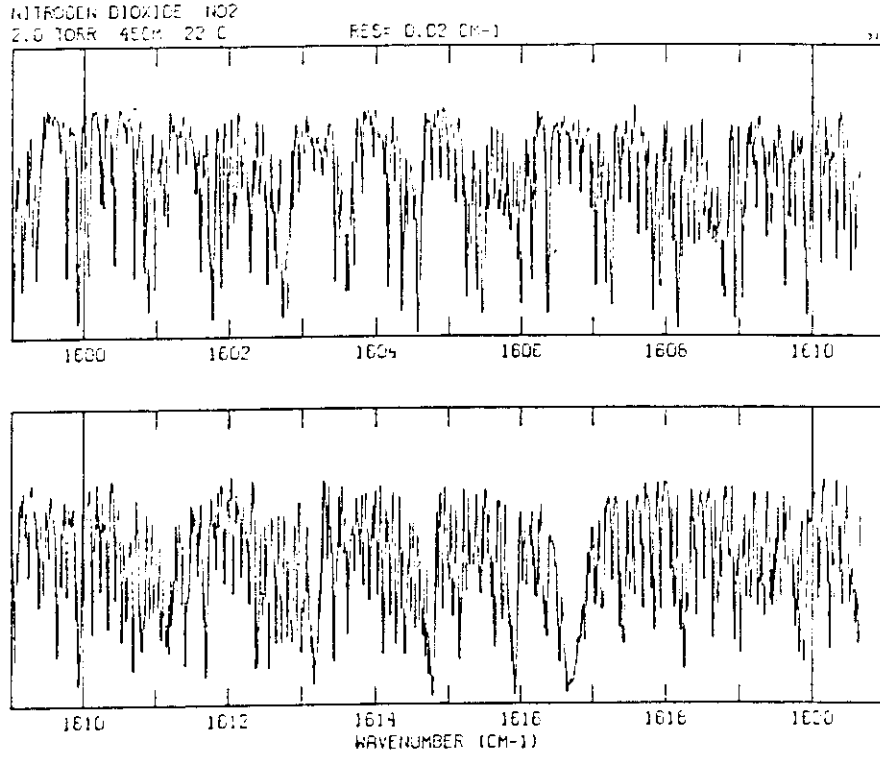
11

Figure 3.7. Nitrogen dioxide spectrum.

$$\tau_\nu(p,\vartheta,q) = exp\left(- \int_0^p k_\nu \frac{q}{g} \sec \vartheta dp\right)$$

$$\tau_\nu'(p,\vartheta,q) = exp\left(- \int_p^{p_s} k_\nu \frac{q}{g} \sec \vartheta dp\right)$$

and is a function of the temperature and gas concentration distribution along the vertical. Subscript s indicates the lower boundaries of the atmosphere.

The first term on the r.h.s. of equation (4.1) describes the radiance emitted from the lower surface, whose skin temperature is T_s, reaching the top of the atmosphere after being attenuated by a factor $(1 - \tau_\nu(p_s, \vartheta))$.

The second term (expressed in eq. 4.2) is the integrated effect of the radiance emitted by each infinitesimal layer dp, centered at pressure p, and depends on mean temperature and gas concentration in the layer and on geometrical path. The emitted radiance is attenuated on its way to the top by the atmospheric layers above, the latter effect being accounted for through the transmittance function τ computed between layer p and the top of the atmosphere.

The third term (eq. 4.3) represents the downward atmospheric radiance reaching the lower surface, reflected by it and reaching the top after being attenuated. This term
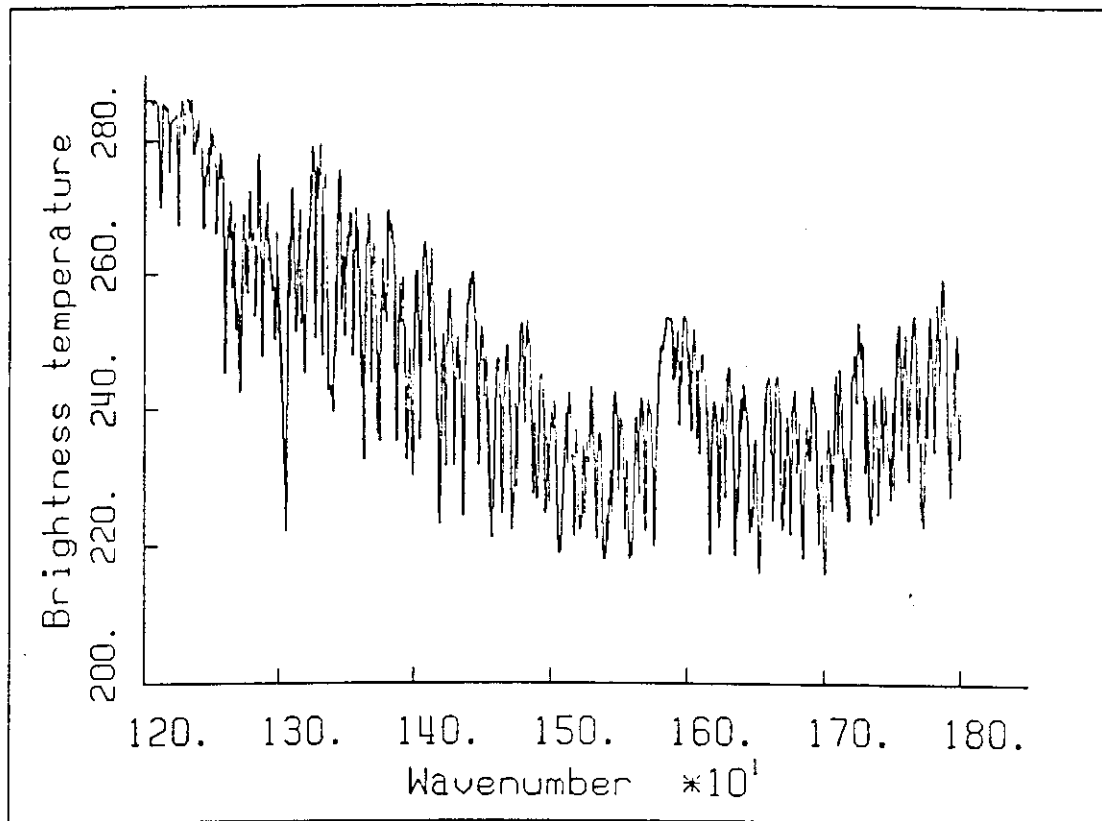
12

Figure 8.8. Emission spectrum of the atmosphere measured at 10 km height with a resolution of approximately half wavenumber. Most of the lines are due to the water vapour vibro-rotational band.

is important when emissivity ε is appreciably different from unity, and can be neglected when discussing infrared radiances while must be accounted for when radiance in the micro-millimeter wavelengths are modelled.

From the discussion follows that the interpretation of the radiance emitted by the atmosphere at a given wavenumber requires, at wavenumber ν, a detailed knowledge of:

   a. spectroscopic properties of all gases radiatively active (which is contained in the term $\tau_\nu(p, \vartheta; T, q)$,

   b. the vertical profile of the concentration for each gas radiatively active (term $q(p)$),

   c. the temperature structure $T(p)$ up to a level where emission phenomena become negligible.

   d. the lower surface radiative properties, that is emissivity and skin temperature.

We can now try to understand the features of the radiance (in terms of T_B) spectrum shown in Fig. 2.1. As already mentioned the active gases in that region of the spectrum are
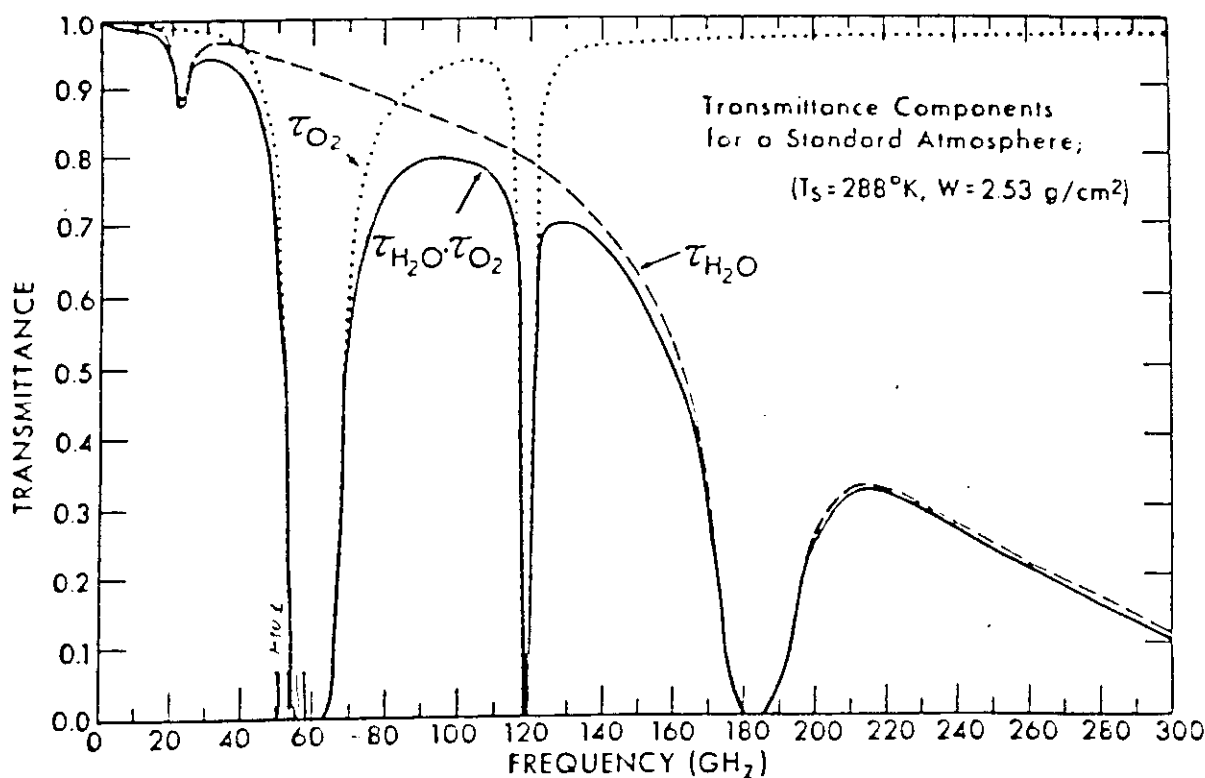
13

Figure 3.9. Transmittances in the micro-millimeter wave region calculated for a path between surface and space for molecular oxigen, water vapour and their product.

CO_2 and O_3 with some contribution from water vapour in the window region. The former of these gases can be considered as uniformly distributed along the vertical. The temperature structure can be approximated by the standard atmosphere with the vertical lapse rate of $\approx -8\,K/km$. Highest values of B_T are observed in the range 800 to 1000 and 1080 to 1120 cm^{-1}, the so-called infrared window region, since the radiation emerging at the top of the atmosphere originates primarily from the (warm) earth surface. Skin temperature can be derived from the hottest points in the curve giving a value of $\approx 283\ K$. In the ozone absorption bands, around 1040 cm^{-1}, radiation emitted by the troposphere is partly absorbed by the layers above while strongest emission, occurring in the most absorptive portions of the band, takes place in the stratosphere, where the largest ozone concentration is found. Since the temperature in the stratosphere is, generally, lower than at the ground lower B_T values are observed. Lowest B_T values are measured in the strongest absorption region of carbon dioxide, from 660 to 680 cm^{-1} since, at these wavenumbers radiation emitted by atmospheric layers close to the ground (and relatively warm) is completely absorbed on its way mid-troposphere. Since CO_2 is almost uniformly mixed along the vertical in the atmosphere, only radiation emitted in the upper tropospheric layers, which are relatively cold, reaches space and therefore the measured brightness temperature is

14

low.

From this brief discussion appears therefore that a series of monochromatic measurements of the emitted upwelling radiance, distributed from the center to the wings of an absorption band, contains intermixed information on the vertical temperature and concentration structure. In any case the relation between radiance, temperature and concentration is highly nonlinear as shown formally by equation (4.1).

There are a number of complications in the practical application of equation (4.1) to remote sounding, some of which will now be briefly discussed.

The measured radiance is not monochromatic but an integral over a substantial bandwidth, required to reach necessary signal–to–noise ratios. Todays radiometers, developed for sounding purposes, use interference filters to select any spectral channel. The typical bandwidth (total width at half power) for these filters is about 10 to 15 cm^{-1}, in the wavelength range we are considering. To understand the effect of integrating radiance according to typical filter response function two spectra are compared in Fig. 4.1 and 4.2, the first showing a small fraction of the spectrun in Fig. 2.1 and the second a smoothed spectrum obtained with a triangular filter function whose bandwith is 10 cm^{-1}. It is evident that the effect is to obtain averages of upwelling radiance coming from different layers of the atmosphere since the informations coming from many absorption lines are effectively integrated. Althought, strictly speaking, monochromatic radiances cannot be measured (at the very end Heisemberg principle poses some fundamental limitation to monochromaticity), measuring radiances over spectral channels whose width is around 10 cm^{-1} influences retrieval quality.

The worst limitation to the use of equation (4.1) is due to the fact that even shallow clouds are opaque to infrared radiation. With the exception of thin cirrus, clouds act as a blackbody effectively masking all radiative information coming from below cloud top. Since the typical horizontal dimension for an infrared sounder field of view ranges from several km to several tens of km, to collect enough energy to mantain a sufficiently high signal–to–noise ratio, a completely clear atmosphere over the field of view of a sounding instrument is a rarity, expecially in meteorologically active areas where temperature profiles are most needed for accurate weather forecasting. In the microwave, although scattering by non-precipitating clouds is almost negligible, scattering due to precipitation makes a noticeable contribution to microwave radiance, hence calculaticn of temperature without accounting for the scattering results in large errors. These effects are enhanced when millimiter–wave radiometers, as the 183 GHz radiometer, which can be used to derive water vapour profile, are used to sound the atmosphere. Uncertainties caused by clouds are the greatest source
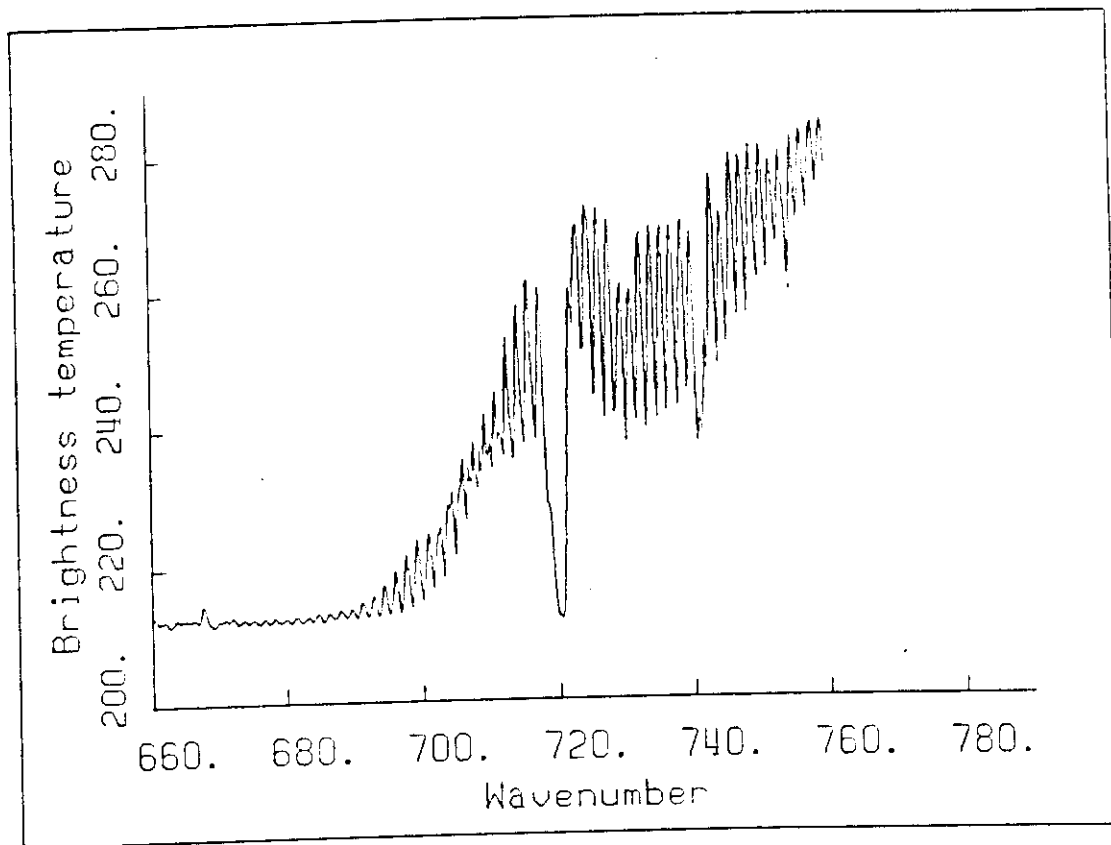
Figure 4.1 Brightness temperature spectrum in t.ie high frequency side of carbon dioxide vibro-rotational band measured with a resclution of about half wavenumber.

of error in remote sensing of the lower and middle atrosphere and will be treated elsewhere in the Course.
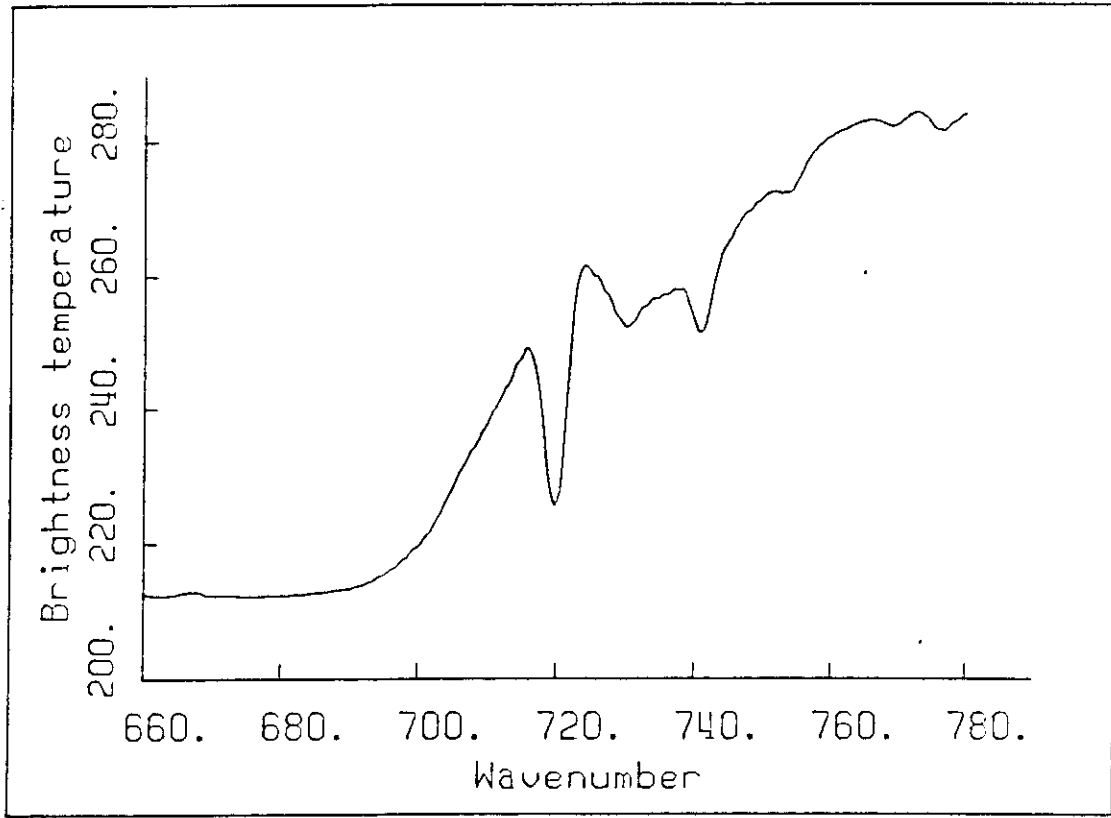
Figure 4.2 Smoothed spectrum of Fig. 4.1 obtained with a triangular filter function of bandwith 10 wavenumbers.

5. The inverse problem.

In spectral region where the transmittance from the ground to the top of the atmosphere is close to zero, equation (4.1), which models the radiance measured from a satellite, can be written (for a vertical path)

$$L_\nu = \int_{p_s}^{0} B_\nu(T) \frac{\partial \tau_\nu}{\partial \ln p} \, d\ln p \tag{5.1}$$

or

$$L_\nu = \int_{0}^{p_s} B_\nu(T) W(T,q) \, d\ln p \tag{5.2}$$

The second equation points out that the term $\partial \tau_\nu / \partial \ln p$ can be interpreted as a *weighting function* W since it determines the contribution of layer p to the radiance reaching the top of the atmosphere. It is therefore instructive to determine the form of the weigthing function appropriate for a single wavenumber chosen in the wing of a collisionally broadened spectral line. The condition for collision broadening means that the halfwidth of the spectral line is greatly enhanced with respect to the "natural" halfwidth (connected to the uncertainty principle) due to interaction between molecules, which modifies to some

17

extent the moment of inertia and/or the vibrational frequencies, giving rise to absorption or emission at further distance from the line center than in an unperturbed condition.

For a single collision broadened spectral line of strength S the variation of absorption coefficient k with frequency is given by the Lorentz profile

$$k_\nu = \frac{S}{\pi} \frac{\alpha}{(\tilde{\nu} - \tilde{\nu}_0)^2 + \alpha^2} \qquad (5.3)$$

$$S = \int_0^\infty k_\nu d\nu$$

where $\tilde{\nu}_0$ is the frequency of the umperturbed monochromatic line, α is the half width of the line which can be written

$$\alpha = \alpha_0 \frac{p}{p_0} \left(\frac{T_0}{T}\right)^{1/2}$$

where α_0 id the half width at standard pressure and temperature. Far from the center of the spectral line so that $(\tilde{\nu} - \tilde{\nu}_0)^2 \gg \alpha^2$ the absorption coefficient is linearly dependent on pressure. The transmittance τ_ν for a vertical path from level p to space can therefore be written as

$$\tau_\nu = \exp\left(-\int_0^p \frac{S\alpha_0}{\pi(\tilde{\nu} - \tilde{\nu}_0)^2 p_0} \left(\frac{T_0}{T}\right)^{1/2} \frac{q}{g} p\,dp\right)$$

Since CO_2 is uniformly mixed in the vertical so that q is nerly independent on p and the term $(T_0/T)^{1/2}$ is close to unity in any case $((300/220)^{1/2} \approx 1.17)$ we may write

$$\tau_\nu = \exp\left(-\beta \int_0^p p\,dp\right) = \exp\left(-\beta p^2/2\right)$$

where β is a constant depending on wavenumber and concentration of absorber. The weighting function can now be written as:

$$W = 2\left(\frac{p}{p_m}\right)^2 \exp\left(-\left(\frac{p}{p_m}\right)^2\right) \qquad (5.4)$$

This function is shown in Fig 5.1.

The value of p_m is the level at which the weighting function attains its maximum value, i/e the one most contributing to the measured radiance from space and depends on the particular wavenumber chosen. The functional form in equation (5.4) represents the best that can be done as far as definining the region of origin of the radiance. Measurements performed at different wavenumbers will have weighting functions peaking at different levels but partly overlapping.
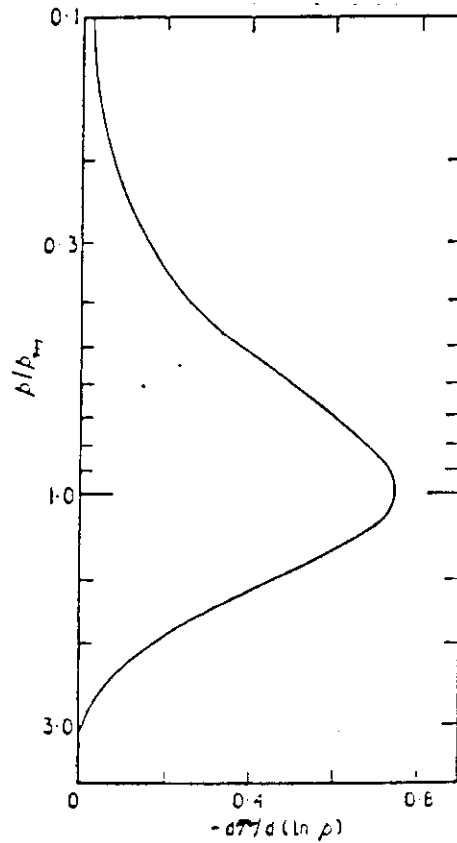
18

Figure 5.1

Idealized monochromatic weighting function for a wavenumber in the wing of a collision broadened spectral line.

Since the width of lines in the vibro–rotational band of CO_2, for example, varies from about 0.1 to 0.001 cm^{-1} depending on pressure, an instrument would need a resolution of 0.1 in the wings and 0.001 cm^{-1} near to the center in order to possess a weighting function like in equation (5.4). As already pointed out however the spectral bandwidth of current sounders ranges around 10 cm^{-1} and the contribution of a great number of lines is effectively averaged. This implies broader weighting functions and a smearing of the contribution from specific layer to total radiance. However most of the energy emitted to space is originated in the spectral regions far from the line centers, since radiation emitted close to them is affected by stronger absorption by the layers above on its way to space. Hence, at the end, the decrease in performance in not very large.

An example of real weighting functions is given in Table 5.1 where the spectral channels of an operational instrumental set, The Tiros Operational Vertical Sounder (TOVS) are defined with their expected (and possibly extracted) information. The today version of TOVS consists of two distinct instruments, the HIRS/2 second version of the High

19

resolution Infrared Radiation Sounder, an infrared interference filter radiometer, and the Microwave Sounding Unit designed to help reducing the cloud effect on infrared radiances. The "energy" weighting functions, for each spectral channel, drawn in Fig. 5.2, are defined as $W_E = B(T)W$ and are normalized so that the peak value is unity.

Table 5.1

Characteristics of TOVS sounding channels.

HIRS Channel number	Channel central wavenumber	Central wavelength (μm)	Principal absorbing constituents	Level of peak energy contribution	Purpose of the radiance observation
1	668	15.00	CO_2	30 mb	Temperature sounding. The 15-μm band channels provide better sensitivity to the temperature of relatively cold regions of the atmosphere than can be achieved with the 4.3-μm band channels. Radiances in Channels 5, 6, and 7 are also used to calculate the heights and amounts of cloud within the HIRS field of view
2	679	14.70	CO_2	60 mb	
3	691	14.50	CO_2	100 mb	
4	704	14.20	CO_2	400 mb	
5	716	14.00	CO_2	600 mb	
6	732	13.70	CO_2/H_2O	800 mb	
7	748	13.40	CO_2/H_2O	900 mb	
8	898	11.10	Window	Surface	Surface temperature and cloud detection.
9	1028	9.70	O_3	25 mb	Total ozone concentration
10	1217	8.30	H_2O	900 mb	Water vapor sounding. Provides water vapor corrections for CO_2 and window channels. The 6.7-μm channel is also used to detect thin cirrus cloud
11	1364	7.30	H_2O	700 mb	
12	1484	6.70	H_2O	500 mb	
13	2190	4.57	N_2O	1000 mb	Temperature sounding. The 4.3-μm band channels provide better sensitivity to the temperature of relatively warm regions of the atmosphere than can be achieved with the 15-μm band channels. Also, the short-wavelength radiances are less sensitive to clouds than those for the 15-μm region.
14	2213	4.52	N_2O	950 mb	
15	2240	4.46	CO_2/N_2O	700 mb	
16	2276	4.40	CO_2/N_2O	400 mb	
17	2361	4.24	CO_2	5 mb	
18	2512	4.00	Window	Surface	Surface temperature. Much less sensitive to clouds and H_2O than the 11-μm window. Used with 11-μm channel to detect cloud contamination and derive surface temperature under partly cloudy sky conditions. Simultaneous 3.7- and 4.0-μm data enable reflected solar contribution to be eliminated from observations
19	2671	3.70	Window	Surface	
20	14367	0.70	Window	Cloud	Cloud detection. Used during the day with 4.0- and 11-μm window channels to define clear fields of view.

MSU	Frequency (GHz)	Principal absorbing constituents	Level of peak energy contribution	Purpose of the radiance observation
1	50.31	Window	Surface	Surface emissivity and cloud attenuation determination.
2	53.73	O_2	700 mb	Temperature sounding. The microwave channels probe through clouds and can be used to alleviate the influence of clouds on the 4.3- and 15-μm sounding channels
3	54.96	O_2	300 mb	
4	57.95	O_2	90 mb	

The spectral location of some of the TOVS channel is shown in Fig. 5.3 where the channels are simplified as having a triangular filter function. The drawing, together with the preceding discussion exemplifies the status of the art with regard to operational instrumentation and the margins of improvement possible with future generation sounding instruments.
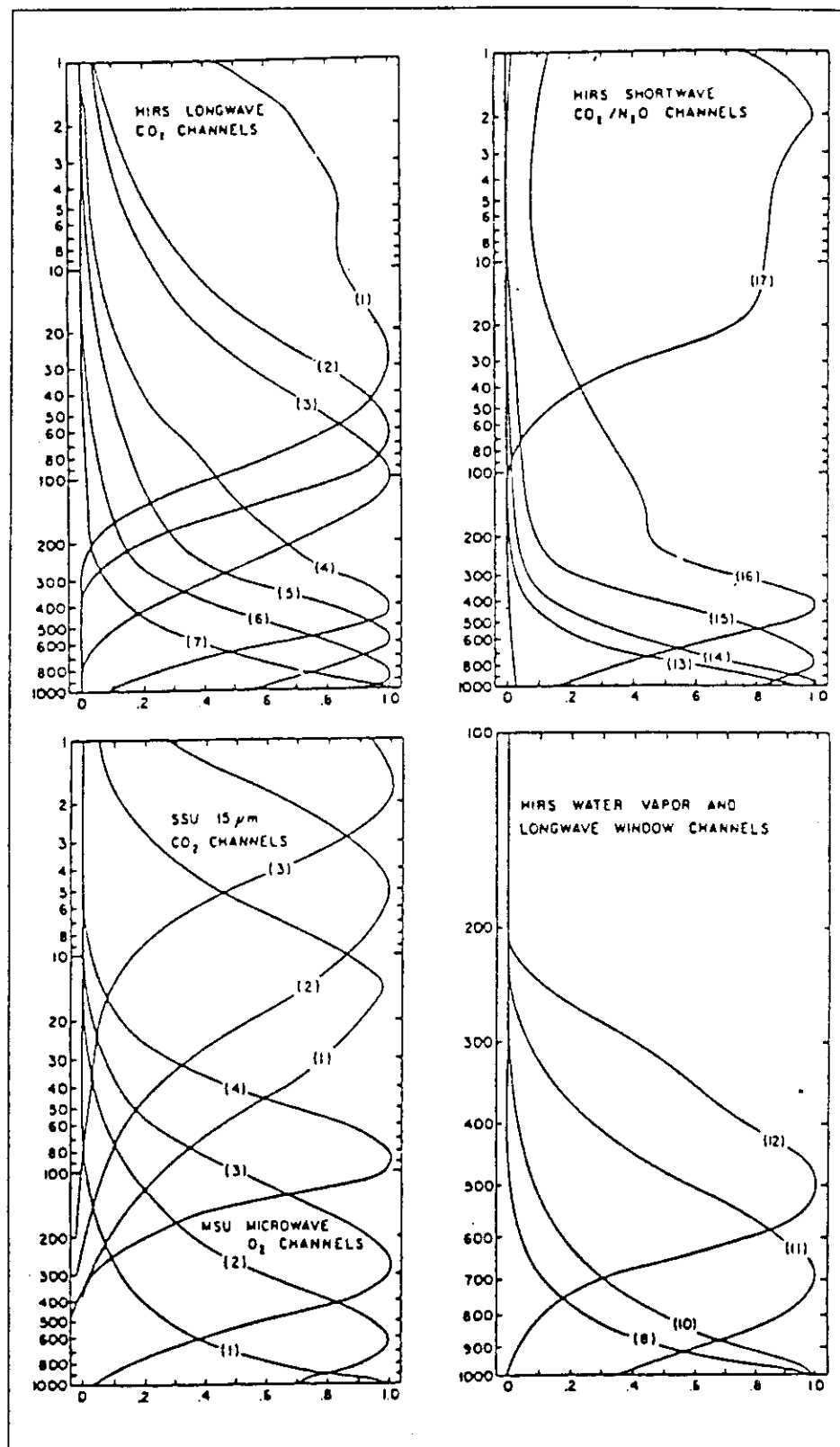
20

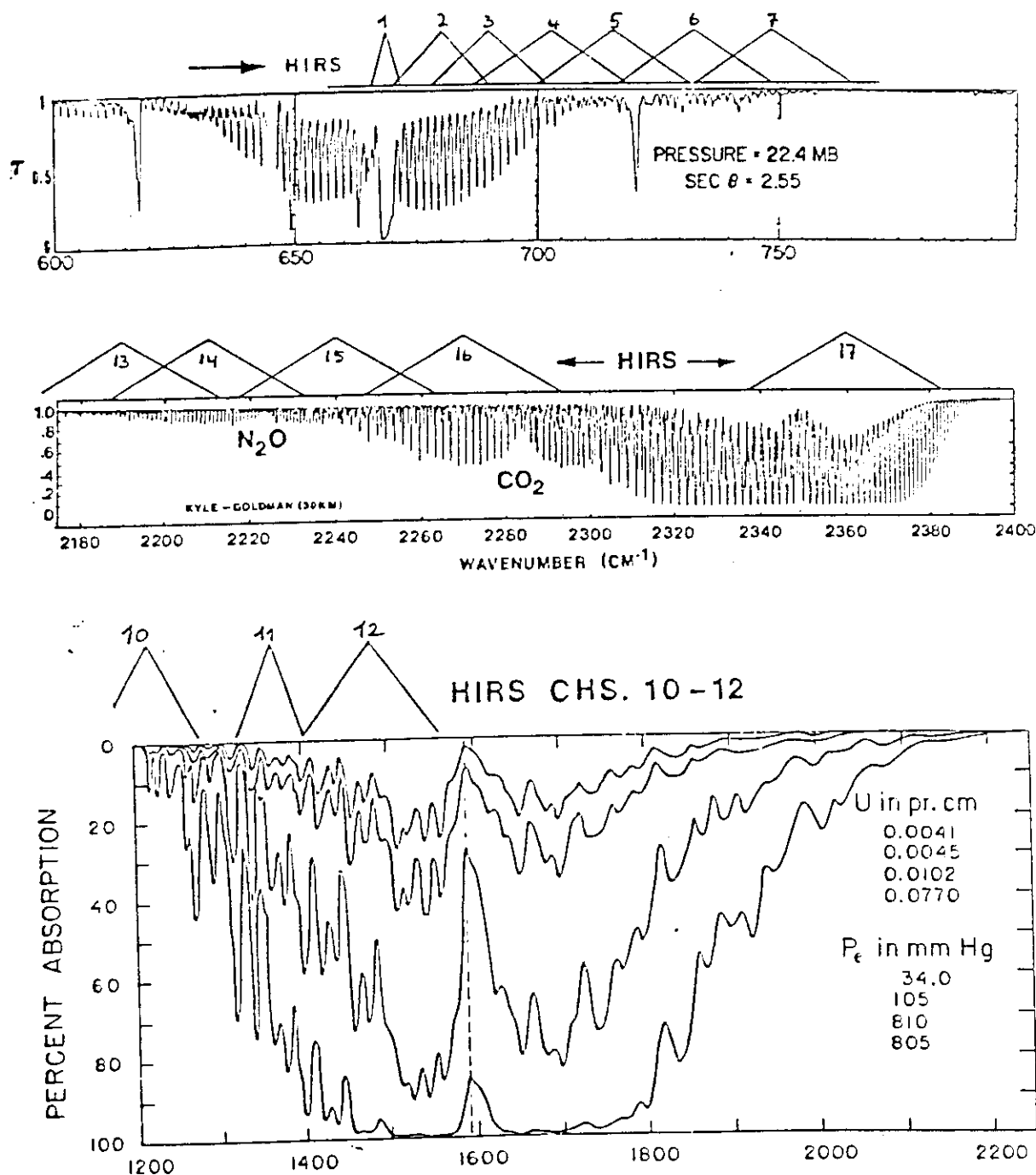**Figure 5.2** TOVS normalized energy weighting functions.

Figure 5.3 Location of some of the channels of TOVS.

7. Bibliography

— S. Twomey, 1977, *Introduction to the Mathematics of Inversion in Remote Sensing and Indirect Measurements*, Elsevier Scientific Publishing Company, New York.

— J.T. Houghton, F.W. Taylor and C.D. Rodgers, 1984, *Remote Sounding of Atmo-*

spheres, Cambridge Planetary Science Series, Cambridge University Press.

— Kuo–Nan Liou, 1980, *An Introduction to Atmospheric Radiation*, Academic Press Inc.

— E. Mc Cartney, 1983, *Absorption and Emission by Atmospheric Gases: The Physical Processes*, John Wiley & Sons.